PID controllers performance on dual axis tracking with tetrahedron based sensor

Andri Novandri[1], Melinda[*2], Yuwaldi Away[3]
Magister of Electrical Engineering, Syiah Kuala University, Indonesia[1]
Department of Electrical Engineering, Syiah Kuala University, Indonesia[2]
Department of Electrical Engineering, Syiah Kuala University, Indonesia[3]

Abstract
This study compares control systems applied to a dual-axis tetrahedron-based sensor tracker. A tetrahedron-based sensor is a tracking sensor that can detect the coordinates of a light source. This study aims to determine a control system that can control sensors with high accuracy and precision and has a fast-tracking ability. Tests are carried out periodically by providing light at certain coordinates. After carrying out the testing and analysis process, it is concluded that the P controller is a better control system than the other controllers. This controller can control sensors with high accuracy and precision compared to PI, PD, and PID control systems. The P controller can also control the sensor to move towards the light coordinates with a travel time of 1.6 seconds on the X-axis and 3.1 seconds on the Y-axis, with a MAE value of 1.1 on the X-axis and 0.3 on the Y-axis. While the RSME value obtained is 1.33 on the X-axis and 0.55 on the Y-axis.

1. Introduction

The sun tracker is a technology that can detect the coordinates of the position of the sun's light. The sensor used in the sun tracker is a tetrahedron-based sensor which is a tracking sensor in the form of a geometric tetrahedron. The sensor captures light and then processes it to determine the light source's position. This tetrahedron-based sensor device aims to maximize the electrical energy generated by photovoltaics using three photoresistors mounted on three sides. The principle works by comparing the difference in the light intensity value on each sensor. Through this comparison, the position of the light source can be known. The tracking system can move degrees of freedom by using two actuator units on each axis [1].

PID controller (Proportional Integral Derivative) is a closed-loop feedback control system aiming to correct the error value. The error value is the difference between the measured and expected setpoint values. The PID controller will process the magnitude of the error value to reduce the error value to a minimum until the error value is close to zero. In addition to reducing the error value, the PID controller also increases or decreases the system response time, such as settling time, rise time, and overshoot. To set the response time, it is necessary to tune the three PID parameters. The three PID controller parameters are Proportional Parameters (P), Integral Parameters (I), and Derivative Parameters (D). These parameters are in charge of controlling the stability of the system based on the response given [2].

Research on the comparison of tracking sensors has been carried out by [3], where in this study, a comparison of the sun tracker in a fixed (static) position with an oriented (dynamic) position that applied a dual-axis was carried out. The results showed that the dynamic tracking system could obtain 30% more solar energy than the static tracking system. In addition, the tetrahedron sensor as a tracking sensor was introduced by [4]. The focus of this study aims to track the position of the sun to obtain coordinate values. Dual-axis sun tracker is also used to maximize the potential of electrical energy converted from solar energy. The technique used in this tetrahedron-based sensor research is to use several light sensors arranged in tetrahedron geometry and photovoltaic, which are driven by two motors or actuators. The results of this study obtained an error value of 1.67 in the condition of one light source, while in the condition of two light sources, an error value of 5.4 was obtained. The results of this study indicate that the resulting error value is still too large. An optimization process needs to be done to minimize the error value. A study [5], a follow-up study, conducted a comparative analysis between PID controllers and FLC. To improve the performance of the sensor-based tetrahedron tracking system, FLC was applied to the dual-axis sun tracker control algorithm along with a comparative study of PID and FLC on the sun tracker based on the tetrahedron geometry sensor. In research [6], two controllers were combined: PID and FLC. Research [7] also researched PID controllers on tracking sensors, with modifications to

the Ziegler Nichols Rules (ZN-PID). As a result, the system response time is faster, and the overshoot is minimal, thus making the tracking system more stable.

The contribution of this study is to discuss the comparative evaluation of the four control systems, namely P, PI, PD, and PID. The controller is applied to a tetrahedron-based sensor tracking system, then tested in stages. The test includes a comparison of system response, accuracy, precision, and the level of errors that occur. System response analysis is done by observing time, angle, and error parameters. Calculate the accuracy and precision value using a confusion matrix by comparing the measurement data with the calculation data. The calculation of the error rate is done by looking at the MAE (Mean Absolute Error) and RSME (Root Square Mean Error) values [8].

2. Research Method

The solar tracking sensor is a system that can move to follow the movement of the sun's position to increase the productivity of electrical energy produced by photovoltaics. The tracking sensor can control the actuator to move on a dual axis, namely on the azimuth axis and on the altitude axis [3], [6], [9]. This sensor device can allow photovoltaics to be more exposed to sunlight so that solar energy will be absorbed more optimally. One form of the sun tracking sensor is shown in Figure 1.

Figure 1. Tracker Sensor [4]

The tetrahedron-based sensor is a light tracking sensor consisting of three light sensors. This sensor works by comparing the values measured on the three light sensors. The sensor used is a photoresistor type, where the value of the resistance on the sensor will change based on the intensity of the light received. The three light sensors are mounted on different sides of the pyramid, as shown in Figure 2(b), with the sensor geometry shown in Figure 2(a). Based on the picture, the S_{ref} point is the 1_{st} sensor position point, the S_{ax1} point is the 2_{nd} sensor position point, and the S_{ax2} point is the 3_{rd} sensor position point. Through the readings of the three sensors, the system can determine the direction of the position of the light source on the azimuth axis and the altitude axis. The comparison between the 1_{st} sensor value as a reference sensor and the 2_{nd} sensor value as a determinant of the sun's position on the altitude axis, while the comparison between the 1_{st} sensor value as a reference sensor and the 3_{rd} sensor value as a determinant of the sun's position on the azimuth axis.
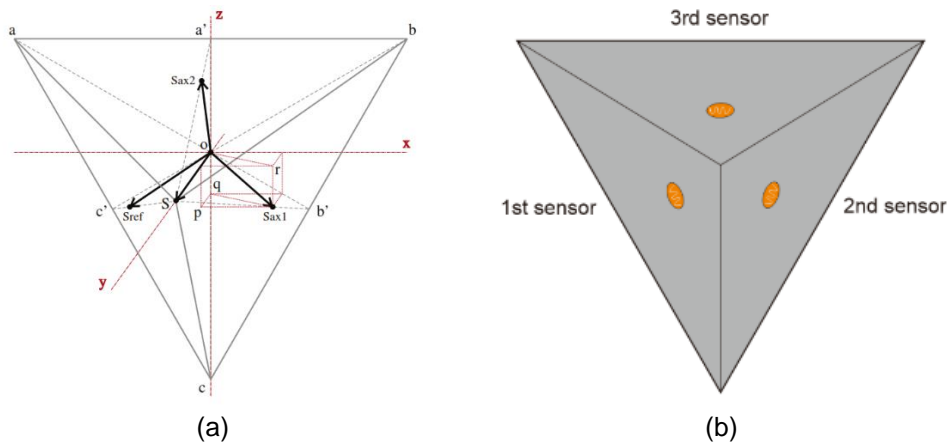

| (a) | (b) |

Figure 2. Tetrahedron-Based Sensor (a) Sensor Geometry, (b) Sensor Position [4]

Figure 3 shows the position of the light source based on Cartesian coordinates in 3 dimensions, where L is the point of the light source. Equation 1 is used to calculate the diagonal distance from the sensor to the light source.

$$r = p \cos(\beta) \tag{1}$$

Meanwhile, to calculate the Cartesian coordinates at point L, Equation 2 is used.
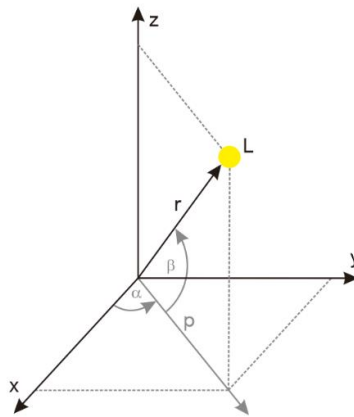

Figure 3. Light Source Cartesian Coordinates

$$\begin{bmatrix} X_L \\ Y_L \\ Z_L \end{bmatrix} = p \begin{bmatrix} \cos(\alpha)\sin(\beta) \\ \sin(\alpha)\sin(\beta) \\ \sin(\beta) \end{bmatrix} \tag{2}$$

PID controller is a feedback control system that can correct the error value between the setpoint value and the measured value. PID control consists of three main parameters: Proportional, Integral, and Derivative. Some systems use one or two parameters to provide appropriate system control. Depending on the desired system application, the PID controller can be a P, PI, or PD controller. This can be achieved by assigning a zero value to the unused parameter [2], [5], [10].

The P controller is a control system that only utilizes the gain value of the P parameter, where in this controller, there is a proportional relationship between the output value and the error value. In simple terms, this type of controller is a product of the proportional constant with its input value [11], [12]. The controlling equation P can be formulated in Equation 3, where $u(t)$ is a transfer function, K_p is a proportional constant value, and $e(t)$ is an error value.

$$u(t) = K_p \, e(t) \tag{3}$$

The PI controller is a control system that utilizes the gain value gain in parameter P and parameter I. This controller has the same characteristics at the rising time and can reduce the overshoot value [13] – [15]. The PI control equation can be formulated in Equation 4, where K_i is the value of the integral constant.

$$u(t) = K_p \, e(t) + K_i \int_0^t e(t) \, dt \tag{4}$$

The PD controller is a control system that utilizes the gain value gain in parameter P and parameter I, where this controller produces a more stable response and smaller overshoot than other controllers. However, errors may still occur because there is no reinforcement in parameter I which acts to accumulate error values that have occurred previously [16], [17]. The PD controller is formulated in Equation 5, where K_d is the value of the derivative constant.

$$u(t) = K_p \, e(t) + K_d \frac{de(t)}{dt} \tag{5}$$

PID controller is a control system that utilizes the gain value for all parameters, where the values for the three parameters will affect the system response and stability and overshoot [18]–[23]. The PID controller equation can be formulated in Equation 6.

$$u(t) = K_p \, e(t) + \, K_i \int_0^t e(t) \, dt + \, K_d \frac{de(t)}{dt} \tag{6}$$

$e(t)$ is the error value in each time unit which is calculated using Equation 7, where $Y_{sp}(t)$ is the setpoint variable, and $Y_m(t)$ is the variable process.

$$e(t) = Y_{sp}(t) - Y_m(t) \tag{7}$$

3. Experimental Methods

This study method uses four types of controllers, namely P controller, PI controller, PD controller, and PID controller. As shown in Figure 4, there are three inputs in the form of light intensity that will track the position of the sun.
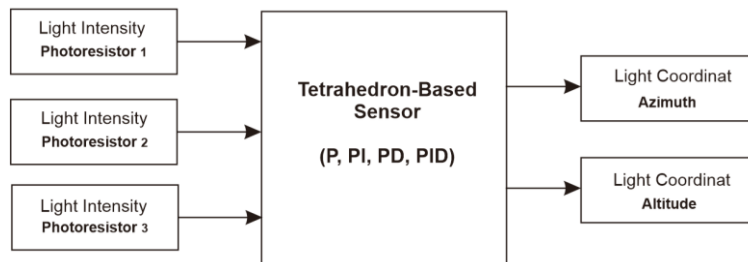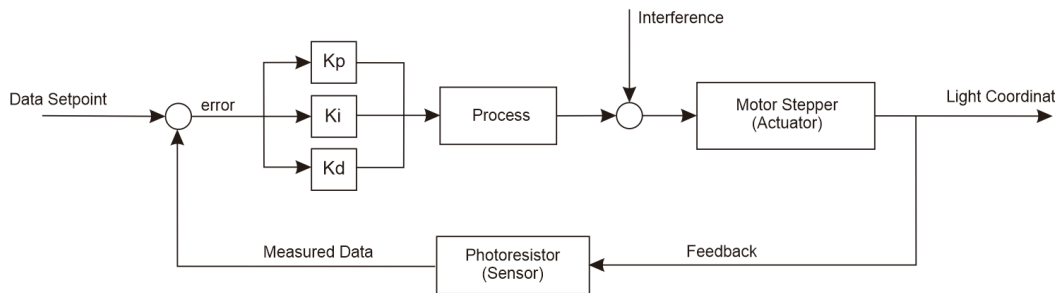

Figure 4. System Block Diagram

Figure 5. Proposed System Work Diagram

The control system used in this study uses three main parameters, namely K_p, K_i, and K_d. These three parameters can be combined to obtain a controller. In using P controller, only K_p value is needed. In the PI controller, two parameter values are needed, namely the value of K_p and K_i. In the PD controller, two parameter values are also needed, namely the value of K_p and K_d. While on the PID controller, three parameter values are needed, namely K_p, K_i, and K_d. These three parameters have their respective functions to maintain stability and response to the system [21], [24], [25]. A tuning process is required to obtain the value of these three parameters. The tuning process is carried out based on the error value contained in the light intensity reading. If there is a difference between the setpoint value and the measured value, the eye has an error value. The processing results will drive an actuator as a stepper motor. The output results will then be fed back (feedback) to compare the value of the output with the setpoint value [22]. The process diagram of the control system is shown in Figure 5.

$$P_{out}(t) = 4.8 \, e(t) \tag{8}$$

$$PI_{out}(t) = 4.8 \, e(t) + \, 1.2 \int_0^t e(t) \, dt \tag{9}$$

$$PD_{out}(t) = 4.8 \, e(t) + \, 0.1 \frac{de(t)}{dt} \tag{10}$$

$$PID_{out}(t) = 4.8\, e(t) + 1.2 \int_0^t e(t)\, dt + 0.1\, \frac{de(t)}{dt} \tag{11}$$

The gain value used in the test is 4.8 at K_p, 1.2 at K_i, and 0.1 at K_d. So that the P controller is obtained in Equation 8, the PI controller is obtained in Equation 9, the PD controller is obtained in Equation 10, and the PID controller is obtained in Equation 11.
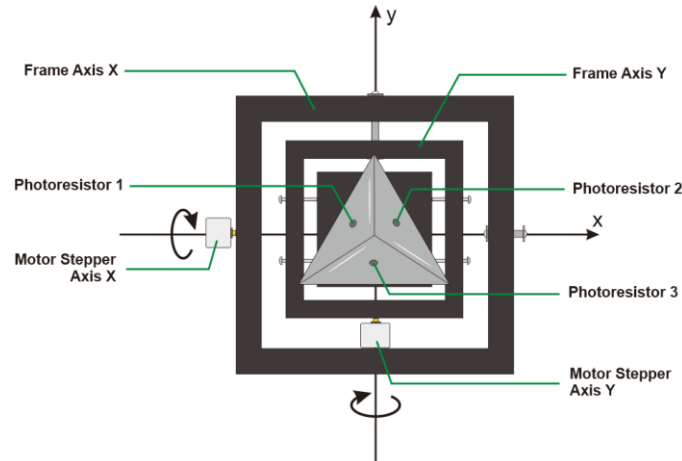

Figure 6. Sensor Configuration

The design of the tetrahedron-based sensor uses two frames that move on different axes. The design form of the tetrahedron-based sensor can be seen in Figure 6. The system consists of three light sensors in the form of a photoresistor as a light tracker and two stepper motors as actuators. The two motors function to move the frame on different axes. The outermost frame functions for driving on the X-axis, while the innermost frame functions for driving on the Y-axis [23], [26].
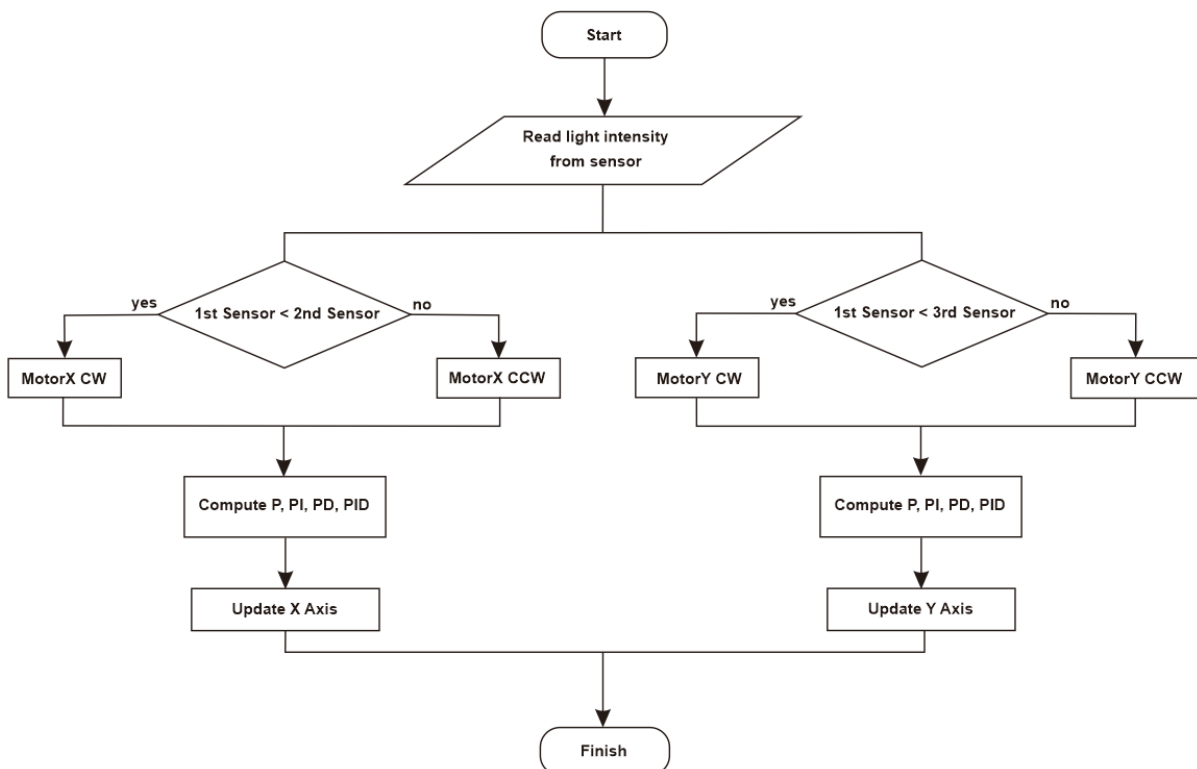

Figure 7. Flowchart System

Figure 7 is a flowchart of a dual-axis tracking system. This system's working principle is based on comparing the light intensity values read by the photoresistor sensor. The comparison value between the 1_{st} sensor and the 2_{nd} sensor determines the direction and angle of rotation of the X-axis motor. In contrast, the comparison value between the 1_{st} sensor and the 3_{rd} sensor determines the direction and angle of rotation of the Y-axis motor. The direction and angle of rotation of the motor are generated through calculations using P, PI, PD, and PID controllers.
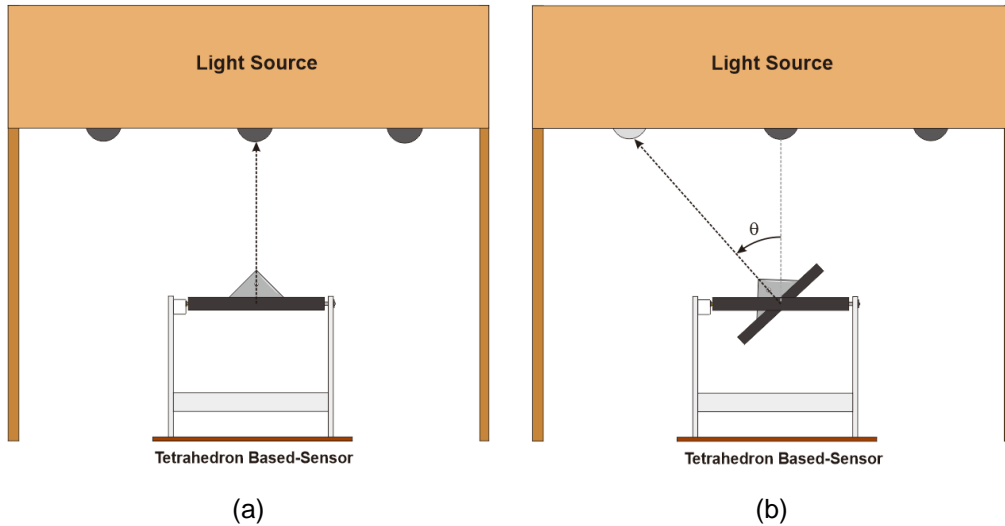

(a)   (b)

Figure 8. Sensor Testing (a) Sensor Position, (b) Sensor Movement
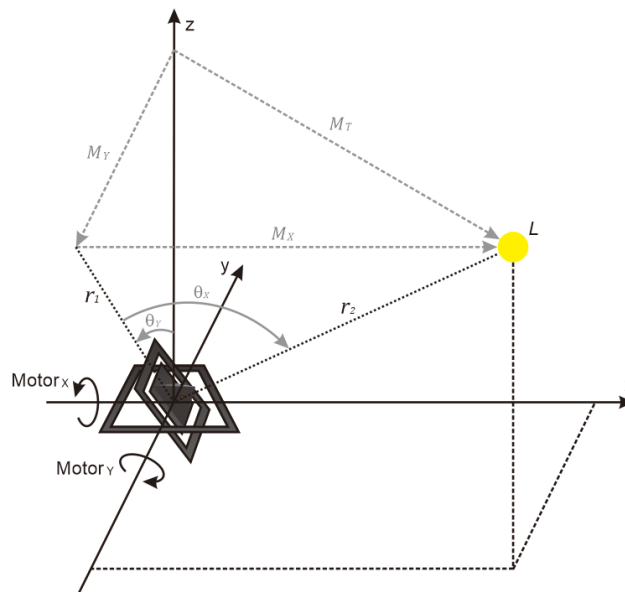

Figure 9. Sensor Work Principle

The tracking system test is carried out using several lights placed above. The lights are flashing alternately randomly. The sensor will move to follow the position of the light so that the motor moves. The sensor testing process is carried out as shown in Figure 8(a), where the sensor position is parallel to the center light. As shown in Figure 8(b), the sensor will move after detecting the presence of light. The angle is the rotation angle of the motor. The movement of the sensor on the dual axis can be seen in Figure 9, where L is the light source. The M_Y line is the sensor movement line on the Y-axis, while the M_x line is the sensor movement on the X-axis. The M_T line is the entire line of sensor movement when both motors are active simultaneously. θ_Y is the rotation angle of the Y-axis motor, while θ_X is the motor rotation angle on the X-axis. Thus, the coordinates of the light source are defined as (θ_X, θ_Y), where θ_X is calculated using Equation 13, while θ_Y is calculated using Equation 12.

$$\theta_Y = \tan^{-1}\left(\frac{M_Y}{z}\right) \tag{12}$$

$$\theta_X = \tan^{-1}\left(\frac{M_X}{r_1}\right) \tag{13}$$

The variable r_1 is the distance between the sensor and the light source on the Y-axis, calculated using Equation 14. In contrast, the variable r_2 is the distance between the sensor to the light source on the X-axis, which can be calculated using Equation 15.

$$r_1 = \frac{M_Y}{\sin \theta_Y} \tag{14}$$

$$r_2 = \frac{M_X}{\sin \theta_X} \tag{15}$$

The tests carried out on the light tracking system produce data in the form of coordinate measurements of the light source. The results are processed using four different control systems. The analysis carried out includes analysis of error values, motor response analysis, and precision accuracy analysis. The error value analysis is carried out to see the comparison of the system in reducing the error value that occurs. Motor response analysis is used to determine the stability and speed of the motor in the face of changes in the direction of light. Precision accuracy analysis was carried out to determine each control system's level of accuracy and precision. The level of accuracy is determined by analyzing the error value using the calculation of Mean Absolute Error (MAE) and Root Square Mean Error (RSME). The MAE value is calculated using Equation 16, and the RSME value is calculated using Equation 17, where n is the number of data, θ_i is the actual angle, and $\hat{\theta}_i$ is the measured angle [27]. The level of precision is determined based on the analysis using the standard deviation. The distance of the data distribution can be known through the standard deviation value so that if the value is large, then the data distribution is far apart. At the same time, if the value is small, then the data distribution is close together. A system that is considered precise is a system that has almost the same data for every measurement made. That means a precise system is a system with a small standard deviation value. To calculate the standard deviation, Equation 18 is used, where σ is the standard deviation, x_i is the value in the i data, n is the number of data, and μ is the average value (mean). To obtain the average value, used Equation 19.

$$MAE = \frac{1}{n}\sum_{i=1}^{n}|\theta_i - \hat{\theta}_i| \tag{16}$$

$$RSME = \sqrt{\frac{1}{n}\sum_{i=1}^{n}(\theta_i - \hat{\theta}_i)^2} \tag{17}$$

$$\sigma = \sqrt{\frac{\sum(x_i - \mu)^2}{n}} \tag{18}$$

$$\mu = \frac{1}{n}\sum_{i=1}^{n}x_i \tag{19}$$

4. Results and Discussion
Based on the results of the tests that have been carried out, some data are obtained for further analysis. The data obtained include motor movement data when the lights are on and motor response data when the light transfer occurs. All of the data is processed, then presented in graphical form, making it easier to analyze.

4.1 Error Rate Analysis
This test is done by testing the system in dark conditions, then given light. Thus, the sensor will move to follow the light source coordinates. Through this movement, it can be seen the changes in the data in reaching the coordinate point. The data is then processed to see the decrease in the error value and is displayed as a graph.

Based on the test results on each controller, a control graph P is generated, as shown in Figure 10. Based on the graph, it can be seen that the X-axis motor takes 1.6 seconds, while the Y-axis motor takes 3.1 seconds. Figure 11 is a graph of the test results for the PI controller. Based on the graph, the X-axis motor takes 1.7 seconds, while the Y-axis motor takes 4.7 seconds. The graph for the PD controller is shown in Figure 12. The graph shows that the movement of the X-axis motor takes 6.2 seconds, and the movement of the Y-axis motor takes 4.8 seconds. The graph of the PID controller is shown in Figure 13. In the graph, the PID controller requires a movement time of 6.6 seconds on the X-axis motor and 6 seconds on the Y-axis motor. The accumulated data is obtained through these data, as shown in Table 1, which compares the time required for the system to reach the minimum error value. The conclusion is that the P control system can reduce the error value quickly, which is 1.6 seconds on the X-axis and 3.1 seconds on the Y-axis. Meanwhile, the PID control system is slow in reducing the error value, which is 6.6 seconds on the X-axis and 6 seconds on the Y-axis.
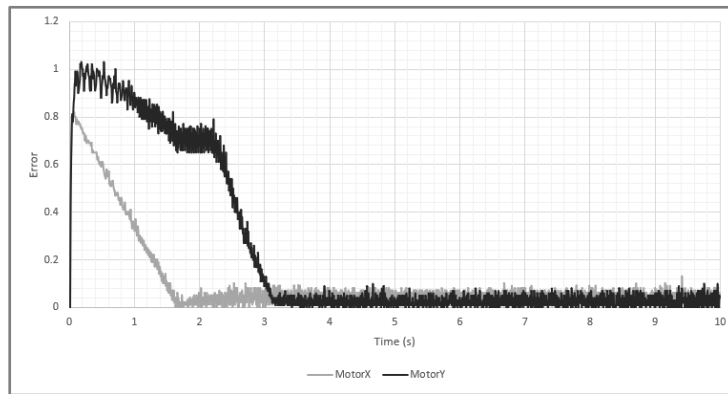

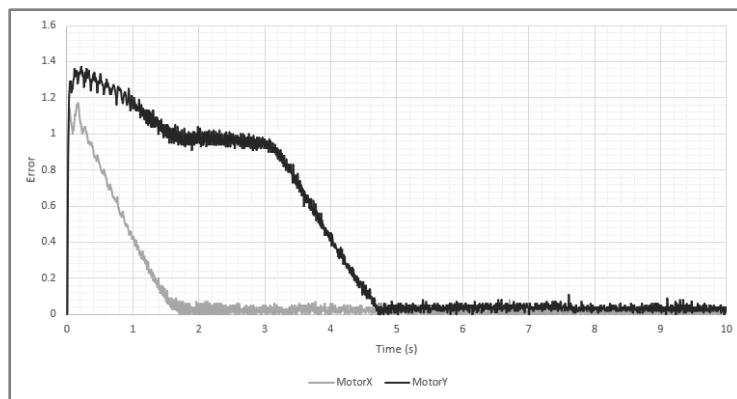*Figure 10. Graph of Error Value Correction on P Controller*
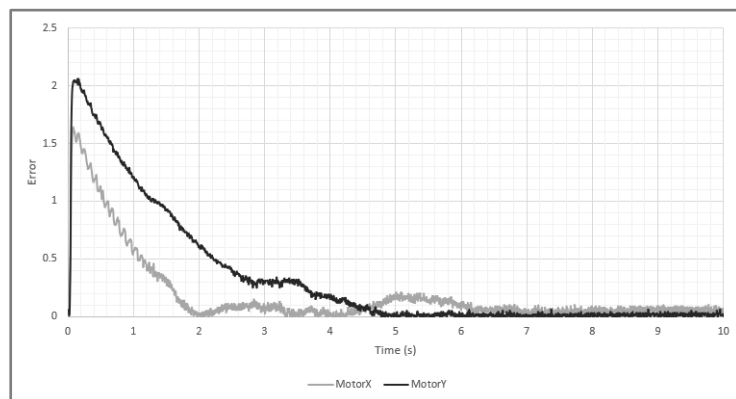

Figure 11. Graph of Error Value Correction on PI Controller

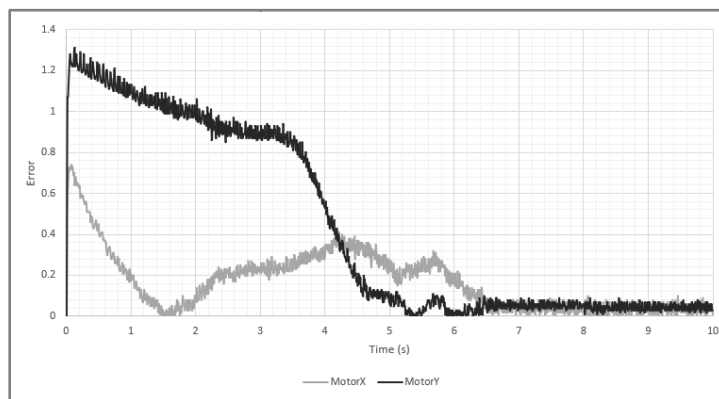*Figure 12. Graph of Error Value Correction on PD Controller*

Figure 13. Graph of Error Value Correction on PID Controller

Table 1. Comparison of Error Time Correction

Controller	Time (s)	
	X-axis	Y-axis
P	1.6	3.1
PI	1.7	4.7
PD	6.2	4.8
PID	6.6	6

4.2 Motor Response Analysis

The test was conducted to analyze the response of the motor on the P, PI, PD, and PID controllers when the light transfer occurs. The testing process is carried out by irradiating the sensor using light at different coordinate positions. The initial position of the sensor is at the coordinates (0°,0°). The test was carried out 3 times with different lamp positions. In light 1, it is at coordinates (-45°, 10°); in light 2, it is at coordinates (10°, -45°); and in light 3, what at coordinates (40°, -25°). Based on the testing process, a graph of the motor movement is obtained every time so that an analysis of the motor response can be carried out on each controller.

Table 2. System Test Results

Controller	Testing	Rise Time (s)		Error (°)		Overshoot (%)		Stability	
		X-axis	Y-axis	X-axis	Y-axis	X-axis	Y-axis	X-axis	Y-axis
P	1	1.4	0.3	1	1	0	0	Yes	Yes
	2	0.9	1.6	0	5	30	0	Yes	Yes
	3	1.6	1	3	0	75	16	Yes	Yes
PI	1	1.4	0.3	3	1	0	0	Yes	Yes
	2	1.7	1.6	10	1	50	4.4	No	No
	3	1.5	0.9	3	1	0	20	No	No
PD	1	2	3	1	0	0	0	No	Yes
	2	2.1	1.2	2	6	90	0	No	No
	3	4	0.9	0	4	0	24	Yes	No
PID	1	1.5	2.2	1	2	0	0	No	Yes
	2	1.7	2	4	3	98	0	No	No
	3	2.7	1	5	1	0	24	Yes	Yes

Comparative data were obtained based on the tests carried out on the P, PI, PD, and PID control systems, as shown in Table 2. Based on the table, it can be seen in the first test that the P control system and PI control have the same rise time value of 1.4 seconds on X-axis motors and 0.3 seconds on Y-axis motors. However, in the error comparison, the X-axis motor on the P controller is smaller than the PI controller, which is 1° on the P controller and 3° on the PI controller. In the second test, the X-axis motor on the P controller has a short rise time of 0.9 seconds, while the rise time on the Y-axis motor is the same as that of the PI controller, which is 1.6 seconds. No error occurs on the X-axis motor for the P control system, but on the Y-axis motor, there is an error of 5°. In the third test, the PI controller has a small rise time value of 1.5 seconds on the X-axis motor and 0.9 seconds on the Y-axis motor. However, the system on the PI controller is unstable on both motors.

Testing the P controller system obtained an average rise time of 1.13 seconds, on the PI controller of 3.33 seconds, on the PD controller of 2.2 seconds, and the PID controller of 1.85 seconds. While the average overshot in the P controller is 20.2%, the PI controller is 12.4%, the PD controller is 19%, and the PID controller is 20.3%. In stability testing, the P control system can achieve stability in every test. Although the average value of overshoot obtained by the P controller is greater than the PI controller and PD controller, the P controller system can maintain its stability and can reach the setpoint value in a short time and with a minimal error value.

4.3 Analysis of Accuracy and Precision

The accuracy and precision analysis process is carried out to determine which system is more accurate and more precise. The calculation method is carried out using the standard deviation. The standard deviation is the distance of the data distribution from the mean value. The larger the standard deviation, the greater the distribution of the data, meaning that the data is less precise. Vice versa, if the standard deviation of the data is small, then the distribution of the data is small, meaning that the data is precise. System accuracy is calculated based on the error rate. The error rate was analyzed using MAE (Mean Absolute Error) and RSME (Root Squared Mean Error). There are 30 sample data from the test results, where the data is taken randomly. Based on these data, an analysis was carried out to obtain comparative data, as shown in Table 3.

Based on the comparison data in Table 3, it can be seen that the P control system has a small standard deviation value, which is 0.76 on the X-axis and 0.47 on the Y-axis. In contrast, the PD control system has a large standard deviation value of 3.56 on the X-axis and 1.67 on the Y-axis. In the analysis of the error rate, the P control system has a low error rate, namely the MAE value of 1.1 on the X-axis and 0.3 on the Y-axis, while the RSME value of 1.33 on the X-axis and 0.55 on the Y-axis. Meanwhile, the PID control system has a large error rate, namely the MAE value of 4.03 on the X-axis and 1.2 on the Y-axis. In contrast, the RSME value is 5.13 on the X-axis and 1.59 on the Y-axis. Thus, it can be concluded that the P control system is a system that is more accurate and precise than the PI, PD, and PID control systems. The PD control system has a low level of precision, while the PID control system has a low level of accuracy.

Table 3. Comparison of System

Controller	Standard Deviation		MAE		RSME	
	X-axis	Y-axis	X-axis	Y-axis	X-axis	Y-axis
P	0.76	0.47	1.1	0.3	1.33	0.55
PI	2.05	1.85	1.57	1.4	2.02	2.29
PD	3.56	1.67	3.73	1.27	4.93	1.75
PID	3.31	1.6	4.03	1.2	5.13	1.59

Studies [4] and [28] are previous studies that also investigated the sensor-based tetrahedron. However, this study uses different sensor designs and mechanisms. The comparison process is carried out in the same way by testing the system using the same lights. A study [4] used a PID control system with an error value of 1.67. This value is higher than the test results on the P controller. This proves that the P control system in this study is better than the previous study. Then in the study [28], which also uses a PID control system, the MAE value is 0.65 on the X-axis and 0.54 on the Y-axis. Comparison with the P control system obtains a smaller X-axis value and a larger Y-axis value. This shows that the Y-axis movement in this study is better than in the previous study.

Figure 14 is a comparison of the response of each control system when a step signal is given. These results indicate that the P and PI controllers are faster and more stable than the other controllers. Both control systems take 2 seconds to reach the reference line from the initial position at 0° to 42° and also take 2 seconds to move from 42° to 0°.
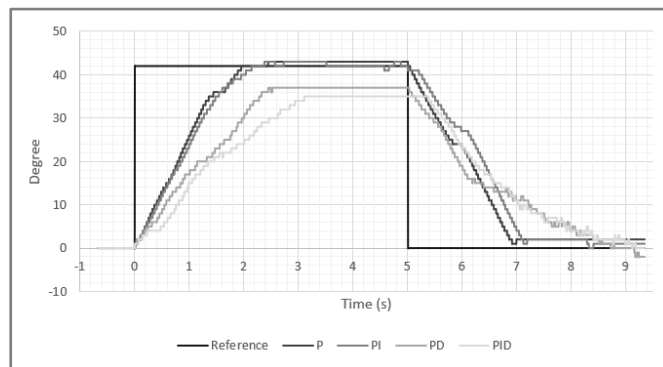
Figure 14. Step response on Each Control System

5. Conclusion

The following results are obtained based on the tests carried out on a dual-axis tetrahedron-based sensor tracking system using P, PI, PD, and PID control systems. The analysis of the error value shows that the P controller can reduce the error value in a short time compared to the other controllers. The time needed to reduce the error value on the X-axis is 1.6 seconds, while it is 3.1 seconds on the Y-axis. The results of the motor response test show that the P control system is smaller, with an average rise time on the X-axis motor of 1.3 seconds and an average rise time on the Y-axis motor of 0.9 seconds. The P controller is more stable, with a small error value based on the test results. In testing accuracy and precision, the P control system has a standard deviation of 0.76 on the X-axis and 0.47 on the Y-axis. The MAE value obtained is 1.1 on the X-axis and 0.3 on the Y-axis. While the RSME value obtained is 1.33 on the X-axis and 0.55 on the Y-axis. These results indicate that the system with P controller is a system that has a high level of accuracy and precision.

Acknowledgement

References

[1] Guan, Y., Gang, C., & Ren, J. (2015). Cooperative solar tracking control of multiple dual-axis PV panels. *7th Chinese Control and Decision Conference (CCDC)*, 4058–4063. https://doi.org/10.1109/CCDC.2015.7162634

[2] Pivoňka, P. (2002). Comparative Analysis of Fuzzy PI/PD/PID Controller Based on Classical PID Controller Approach. *IEEE International Conference on Fuzzy Systems*, 1, 541–546. https://doi.org/10.1109/fuzz.2002.1005048

[3] Doss C.r., J., Kumaravel, M., & Jagadeesh Kumar, V. (2013). A Novel Measurement Technique for Performance Comparison of Sun Tracker Systems. *Conference Record - IEEE Instrumentation and Measurement Technology Conference*, 1156–1160. https://doi.org/10.1109/I2MTC.2013.6555595

[4] Away, Y., & Ikhsan, M. (2017). Dual-axis sun tracker sensor based on tetrahedron geometry. *Automation in Construction*, 73, 175–183. https://doi.org/10.1016/j.autcon.2016.10.009

[5] Away, Y., Rahman, A., Auliandra, T. R., & Firdaus, M. (2018). Performance Comparison between PID and Fuzzy Algorithm for Sun Tracker Based on Tetrahedron Geometry Sensor. *International Conference on Electrical Engineering and Informatics, ICELTICs*, 40–44. https://doi.org/10.1109/ICELTICS.2018.8548837

[6] Gaballa, M. S., Bahgat, M., & Abdel-Ghany, A. G. M. (2018). Self-Tuning of An FLC-PID Controller of A Dual-Axis Sun Tracker Photo-Voltaic Panel Based on Rise-Time-Observer Method. *19th International Middle-East Power Systems Conference (MEPCON)*, 722–727. https://doi.org/10.1109/MEPCON.2017.8301261

[7] Aung, C. A., Hote, Y. V., Pillai, G., & Jain, S. (2020). PID Controller Design for Solar Tracker via Modified Ziegler Nichols Rules. *2nd International Conference on Smart Power and Internet Energy Systems*, 531–536. https://doi.org/10.1109/SPIES48661.2020.9243009

[8] Kumngern, M., & Torteanchai, U. (2014). FDCCII-Based P, PI, PD and PID Controllers. *Fourth International Conference on Digital Information and Communication Technology and Its Applications (DICTAP)*, 415–418. https://doi.org/10.1109/DICTAP.2014.6821722

[9] Rizvi, A. A., Addoweesh, K., Abdelrehman, E.-L., & Al-Ansary, H. (2014). Sun Position Algorithm for Sun Tracking Applications. *Annual Conference of the IEEE Industrial Electronics Society*, 5595–5598. https://doi.org/10.1109/IECON.2014.7049356

[10] Pati, S., Patnaik, M., & Panda, A. (2014). Comparative Performance Analysis of Fuzzy PI, PD and PID Controllers Used in A Scalar Controlled Induction Motor Drive. *International Conference on Circuits, Power and Computing Technologies (ICCPCT)*, 910–915. https://doi.org/10.1109/ICCPCT.2014.7054799

[11] Liu, C., Zhao, F. Y., Hu, P., Hou, S., & Li, C. (2010). P Controller with Partial Feed Forward Compensation and Decoupling Control for The Steam Generator Water Level. *Nuclear Engineering and Design*, 240(1), 181–190. https://doi.org/10.1016/j.nucengdes.2009.09.014

[12] Tan, N. (2009). Computation of Stabilizing PI-PD Controllers. *International Journal of Control, Automation and Systems*, 7(2), 175–184. https://doi.org/10.1007/s12555-009-0203-y

[13] Wang, Y. G., & Shao, H. H. (2000). Optimal Tuning for PI Controller. *Automatica*, 36(1), 147–152. https://doi.org/10.1016/S0005-1098(99)00130-2

[14] Tomei, P. (1991a). A Simple PD Controller for A Robot with Elastic Joints. *IEEE Transactions on Automatic Control*, 36(10), 1208–1213. https://doi.org/10.1109/9.90238

[15] Suruz Miah, M., & Gueaieb, W. (2014). Optimal Time-Varying P-Controller for A Class of Uncertain Nonlinear Systems. *International Journal of Control, Automation and Systems*, 12(4), 722–732. https://doi.org/10.1007/s12555-013-0234-2

[16] Sánchez, J., Visioli, A., & Dormido, S. (2011). A Two-Degree-of-Freedom PI Controller Based on Events. *Journal of Process Control*, 21(4), 639–651. https://doi.org/10.1016/j.jprocont.2010.12.001

[17] Ramirez, H. S. (1991). Nonliniear P-I Controller Design for Switchmode DC-to-DC Power Converters. *IEEE Transactions on Circuit and System*, 38(4), 410–417. https://doi.org/10.1109/31.75397

[18] Tomei, P. (1991b). Adaptive PD Controller for Robot Manipulators. *IEEE Transactions on Robotics and Automation*, 7(4), 565–570. https://doi.org/10.1109/70.86088

[19] Bansal, H. O., Sharma, R., & Shreeraman, P. R. (2012). PID Controller Tuning Techniques: A Review. *Journal of Control Engineering and Technology*, 2(May), 168–176.

[20] Shah, P., & Agashe, S. (2016). Review of Fractional PID Controller. *Mechatronics*, 38, 29–41. https://doi.org/10.1016/j.mechatronics.2016.06.005

[21] Dawson, D. M., Qu, Z., Lewis, F. L., & Dorsey, J. F. (1990). Robust Control for The Tracking of Robot Motion. *International Journal of Control*, 52(3), 581–595. https://doi.org/10.1080/00207179008953554

[22] Sabir, M. M., & Ali, T. (2016). Optimal PID Controller Design Through Swarm Intelligence Algorithms for Sun Tracking System. *Applied Mathematics and Computation*, 274, 690–699. https://doi.org/10.1016/j.amc.2015.11.036

[23] Jia, R., Nandikolla, V. K., Haggart, G., Volk, C., & Tazartes, D. (2017). System Performance of an Inertially Stabilized Gimbal Platform with Friction, Resonance, and Vibration Effects. *Journal of Nonlinear Dynamics*, 2017, 1–20. https://doi.org/10.1155/2017/6594861

[24]   Fauziyah, M., Adhisuwignjo, S., Ifa, L. N., & Afandi, B. F. (2022). DC Motor PID Control System for Tamarind Turmeric Herb Packaging on Rotary Cup Sealer Machine. *Kinetik: Game Technology, Information System, Computer Network, Computing, Electronics, and Control*, *4*(1), 45–54. https://doi.org/10.22219/kinetik.v7i1.1352

[25]   Wu, H., Su, W., & Liu, Z. (2014). PID Controllers: Design and Tuning Methods. *9th IEEE Conference on Industrial Electronics and Applications*, 808–813. https://doi.org/10.1109/ICIEA.2014.6931273

[26]   Abdo, M. M., Vali, A. R., Toloei, A. R., & Arvan, M. R. (2014). Stabilization Loop of A Two Axes Gimbal System Using Self-Tuning PID Type Fuzzy Controller. *ISA Transactions*, *53*(2), 591–602. https://doi.org/10.1016/j.isatra.2013.12.008

[27]   Wang, W., & Lu, Y. (2018). Analysis of the Mean Absolute Error (MAE) and the Root Mean Square Error (RMSE) in Assessing Rounding Model. *IOP Conference Series: Materials Science and Engineering*, *324*(1). https://doi.org/10.1088/1757-899X/324/1/012049

[28]   Azmi, S., Away, Y., & Sara, I. D. (2016). Kajian Aspek Kecepatan dan Ketepatan pada Sun Tracker Dua Sumbu Berbasis Sensor Berbentuk Tetrahedron. *Jurnal Rekayasa Elektro*, *15*(2), 1–9. https://doi.org/10.17529/jre.v15i2.13546